Origins of the sarsen megaliths at Stonehenge

ARCHAEOLOGY

Origins of the sarsen megaliths at Stonehenge

David J. Nash[1,2]*, T. Jake R. Ciborowski[1], J. Stewart Ullyott[1], Mike Parker Pearson[3], Timothy Darvill[4], Susan Greaney[5], Georgios Maniatis[1], Katy A. Whitaker[6,7]

The sources of the stone used to construct Stonehenge around 2500 BCE have been debated for over four centuries. The smaller "bluestones" near the center of the monument have been traced to Wales, but the origins of the sarsen (silcrete) megaliths that form the primary architecture of Stonehenge remain unknown. Here, we use geochemical data to show that 50 of the 52 sarsens at the monument share a consistent chemistry and, by inference, originated from a common source area. We then compare the geochemical signature of a core extracted from Stone 58 at Stonehenge with equivalent data for sarsens from across southern Britain. From this, we identify West Woods, Wiltshire, 25 km north of Stonehenge, as the most probable source area for the majority of sarsens at the monument.

INTRODUCTION

The origins of the stones used to build the monument of Stonehenge and their transportation methods and routes have been the subject of debate among archaeologists and geologists for more than four centuries (*1*–*6*). Two main types of stones are present at the monument (Fig. 1). The smaller "bluestones" have attracted the most geological attention. These stones—which include dolerites, tuffs, rhyolites, and sandstones—are clearly not local to Stonehenge, which stands in an area underlain by Chalk bedrock. Recent studies suggest that the igneous bluestones originated from the Preseli Hills in southwest Wales [e.g., (*7*–*9*)], over 200 km west of the monument, and that the sandstone Altar Stone came from east Wales (*10*). However, with the exception of work by Howard (*11*), no research has been published on the sources of the larger sarsens [a vernacular term for the duricrust silcrete; (*12*)], erected during the mid-third millennium BCE, that comprise the main architecture of Stonehenge (*13*, *14*). Today, only 52 of the original ~80 sarsen stones remain at the monument. These include all 15 stones forming the central Trilithon Horseshoe, 33 of the 60 uprights and lintels from the outer Sarsen Circle, plus the peripheral Heel Stone, Slaughter Stone, and two of the four original Station Stones.

Typical sarsen uprights at Stonehenge have a long-axis length of 6.0 to 7.0 m (including sections below ground) and weigh ~20 metric tons, with the largest reaching 9.1 m (Stone 56) and having an aboveground weight of ~30 metric tons (Stone 54) (*15*). Their size, coupled with the limited occurrence of sarsen boulders on Salisbury Plain today (*16*), has led to the perceived wisdom that these stones were sourced from the Marlborough Downs (Fig. 1B), 30 km to the north of the monument (*17*). This view has prevailed since the writings of the 16th century antiquary William Lambarde (*1*) but is rarely challenged and has never been rigorously tested. It is certainly true that the most extensive spreads of sarsen boulders in Britain today occur on the Marlborough Downs (Fig. 1A). However, given that sarsen was used to construct megalithic monuments in Kent, Dorset, and Oxfordshire [e.g., (*18*)], it is not impossible that these regions could also have supplied stones for Stonehenge. Furthermore, as the distant sources of the bluestones attest, the choice of stone used to construct Stonehenge was far from pragmatic or based simply on local availability (*14*, *19*).

Here, we apply a novel combination of geochemical and statistical approaches, developed and validated on silcretes in southern Africa (*20*, *21*), to determine the provenance of the sarsen stones at Stonehenge. First, we use portable x-ray fluorescence spectrometry (PXRF) to provide an initial chemical characterization of all extant sarsen uprights and lintel stones. The resulting data are analyzed statistically to determine the degree of chemical variability present across the monument. We then undertake inductively coupled plasma mass spectrometry (ICP-MS) and ICP–atomic emission spectrometry (ICP-AES) analyses of (i) samples from a recently rediscovered core drilled through sarsen Stone 58 at Stonehenge and (ii) a representative range of sarsen boulders from across southern Britain. These analyses are used to generate high-resolution chemical signatures for the monument and potential source regions. Comparisons of these signatures allow us to identify the most likely source area for the sarsens at Stonehenge.

RESULTS

Chemical variability within the sarsen stones at Stonehenge

Nondestructive chemical analyses of all 52 sarsens present at Stonehenge were undertaken using PXRF. This involved taking five readings at random positions across each stone, generating 260 analyses for 34 chemical elements (see Materials and Methods; full dataset is provided in data file S1). The PXRF data demonstrate that the sarsens typically comprise >99% silica, with only traces of each of the other major elements (Al, Ca, Fe, K, Mg, Mn, P, and Ti) present. This high purity is in line with the previous analyses of British sarsens [e.g., (*22*–*24*)] and reflects the mineralogy of the stones, which comprise quartz sands cemented by quartz. Ten of the PXRF analyses at the monument record anomalously low Si (see Materials and Methods), which most likely indicates that nonquartz accessory mineral grains were excited by the x-ray beam during data acquisition. These readings are excluded from subsequent statistical investigations.

Linear discriminant analysis (LDA) and Bayesian principal component analysis (BPCA) were used to analyze the PXRF data (see Materials and Methods). BPCA was chosen over standard principal

[1]School of Environment and Technology, University of Brighton, Lewes Road, Brighton BN2 4GJ, UK. [2]School of Geography, Archaeology and Environmental Studies, University of the Witwatersrand, Johannesburg, South Africa. [3]Institute of Archaeology, University College London, 31-34 Gordon Square, London WC1H 0PY, UK. [4]Department of Archaeology and Anthropology, Bournemouth University, Fern Barrow, Poole, Dorset BH12 5BB, UK. [5]English Heritage, 29 Queen Square, Bristol BS1 4ND, UK. [6]Department of Archaeology, University of Reading, Whiteknights, Reading RG6 6AH, UK. [7]Historic England, 4th Floor, Cannon Bridge House, 25 Dowgate Hill, London EC4R 2YA, UK.
*Corresponding author. Email: d.j.nash@brighton.ac.uk

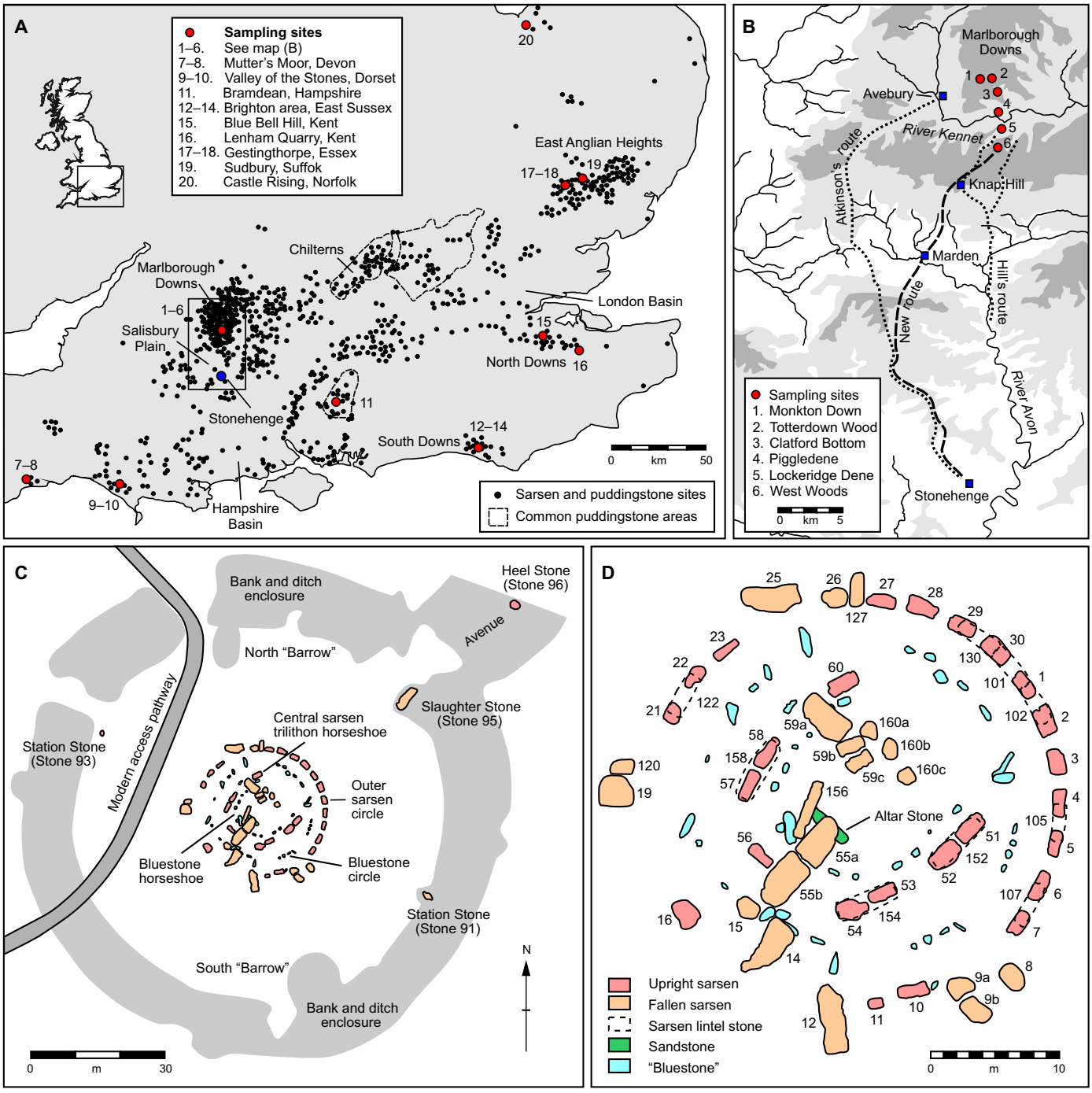

Fig. 1. Stonehenge in context. (**A**) Distribution of silcrete boulders across southern Britain, including sarsens and conglomeratic variants known as puddingstone [data from (*16*, *22*, *28*, *46*, *47*)]. (**B**) Sampling sites and topography in the Stonehenge-Avebury area [areas in pale gray at 100 to 175 m above sea level (asl), and those in dark gray at 175 to 270 m asl], along with proposed transportation routes for the sarsen stones. (**C**) Plan of Stonehenge showing the area of the monument enclosed by earthworks plus numbered peripheral sarsen stones. (**D**) Detail of the main Stonehenge monument showing the remaining bluestones and numbered sarsen stones.

component analysis (PCA) as the latter has limited utility for zero-inflated or incomplete datasets (*25*), both common issues in geochemical studies where many elements are at such low concentrations that they fluctuate close to or below instrumental detection limits. For all statistical analyses, data for the following elements were omitted—Si, Ca, and Fe [to avoid potential anomalies caused by the introduction of iron and replacement of Si by Ca during late-stage diagenesis and subaerial weathering; (*23*)], and Co, Cd, Se, Sb, and Sn (which were below detection limits in all PXRF readings).

Exploratory LDA models indicate significant clustering of the PXRF data (model accuracy, ~0.25), with most analyses falling within a single cluster (Fig. 2A). We define a sarsen as being statistically

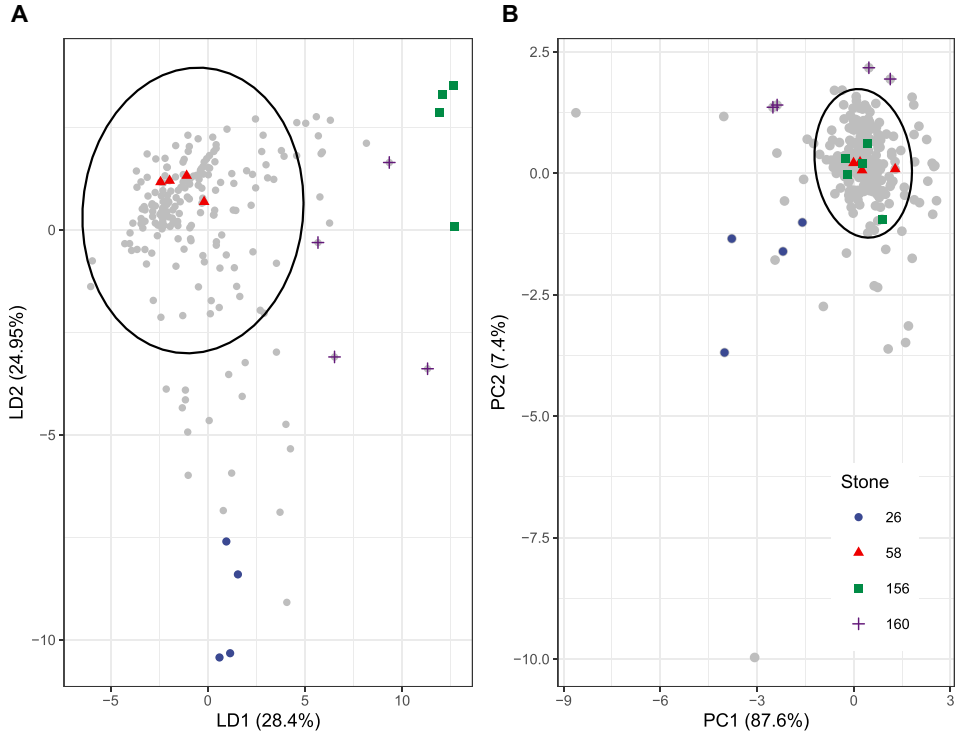

Fig. 2. Results of the statistical analysis of PXRF data from all 52 sarsen stones at Stonehenge. (**A**) Results of linear discriminant analysis and (**B**) Bayesian principal component analysis. LD1, linear discriminant 1; PC1, principal component 1. Only selected sarsens discussed in the text are highlighted in each graphic. Covariance of the first six principal components from the BPCA is shown in fig. S1, with the respective element loadings in table S1 (see figs. S2 and S3 for BPCA results for other stones, and figs. S4 and S5 for BPCA results according to the main structural components at the monument). Ellipsoids indicate the 95% normal confidence ellipses.

different from this cluster only where all individual PXRF analyses for the stone fall beyond the 95% confidence ellipsoid. Using this criterion, three sarsens—upright 26 and lintels 156 and 160—can be identified as chemically distinct from the rest of the monument.

The LDA results are supported by the outcomes of the BPCA (Fig. 2B). The BPCA model performs very well in terms of explaining the variability of the PXRF dataset (PC1 to PC2, $R^2 = 0.95$; covariance of the first six principal components is shown in fig. S1, with respective element loadings in table S1). Here, the majority of analyses, including those from lintel 156, fall within a well-defined cluster enclosed by an approximately circular loading. All analyses of upright 26 and lintel 160 fall beyond the 95% confidence limit. Results for other sarsens are presented in fig. S2 (Stones 1 to 30) and fig. S3 (Stones 51 to 158). The BPCA results further indicate no geochemical difference between the separate structural elements of Stonehenge (i.e., the Trilithon Horseshoe, Sarsen Circle, and peripheral stones; fig. S4) nor between sarsen uprights and lintel stones (fig. S5).

In summary, the results of LDA and BPCA show that 50 of the 52 remaining sarsens at Stonehenge share a similar geochemistry. Upright 26 and lintel 160 have distinctly different chemistries, both from each other and from the rest of the sarsens at the monument. While exploratory LDA results suggest that lintel 156 may also have a different chemistry, the more statistically powerful, unsupervised BPCA method indicates that the chemistry of this stone is instead closer to that of most other sarsens at Stonehenge.

Chemical composition of sarsen Stone 58 at Stonehenge

During a restoration program at Stonehenge in 1958, three sarsen stones that fell in 1797 were reerected (uprights 57 and 58 and lintel 158 from the Trilithon Horseshoe; Fig. 1D). Details of the conservation work are provided in two unpublished reports held in the Ministry of Works registry archive (Registry Files AA 71786/2R Part 2,9 and Part 2,16). In the course of this work, longitudinal fractures were noted through Stone 58. After reerection, to conserve the integrity of the upright, three horizontal holes were drilled through the full thickness of the stone by Van Moppes (Diamond Tools) Ltd. of Basingstoke (UK). Metal ties were inserted into these holes and secured using recessed metal bolt heads, with the holes at the surface of the upright filled using plugs of sarsen.

The drill cores from Stone 58 were assumed "lost." However, in 2018, one complete (1.08 m long, 25-mm diameter) but fragmented core was returned to the United Kingdom from the United States by Robert Phillips, a former employee of Van Moppes who was on-site during the drilling operations. Following publicity generated by the return of this core (referred to here as the "Phillips' Core"), a 0.18-m section of a second core was located at the Salisbury Museum in 2019. The whereabouts of the third core and the remainder of the second core are currently unknown.

With permission from English Heritage, a 67-mm-long section of the Phillips' Core (from between 0.29 and 0.36 m along the core length) was sampled. This involved cutting the core fragment in half lengthways, with one semicylinder retained by English Heritage and the other cut into three equal-sized samples for petrological, mineralogical, and geochemical investigations; these included high-resolution whole-rock ICP-MS and ICP-AES analyses (see Materials and Methods; full dataset is provided in data file S1).

The statistical results in Fig. 2 indicate that Stone 58 falls near the centers of the main clusters identified by both LDA and BPCA

analyses. By inference, the ICP-MS/-AES data from this stone can therefore be considered as chemically representative of the majority of sarsens at Stonehenge. Under standard major element rock classification schemes (*26*), the Phillips' Core samples would be considered as quartz arenites. The ICP-MS/-AES data show that Stone 58 is silica rich [$SiO_2 \geq 99.7$ weight % (wt %)], with very little variation in major element chemistry (0.05 to 0.06 wt % Al_2O_3, 0.01 wt % CaO, 0.09 to 0.12 wt % Fe_2O_3, and 0.06 wt % TiO_2). The remaining major element oxides (Na_2O, MgO, K_2O, MnO, and P_2O_5) are at or below instrumental detection limit (0.01 wt %) in each of the three samples. The consistency between the ICP-MS/-AES and PXRF major element data for Stone 58 is self-supporting.

Comparison of the chemistry of Stone 58 with potential source areas

Sarsen stone is not found as a continuous geological stratum in southern Britain. Rather, it most likely formed as patchy groundwater silcrete lenses within areas of sandy sediment (*23*) and, following erosion and local transport by geomorphological processes (*27*), now occurs as unevenly distributed scatters of boulders resting mainly on the Chalk (Fig. 1A) (*22*, *28*). The original thickness of each sarsen deposit is unknown. However, the dimensions of the largest megaliths at Stonehenge and Avebury (Fig. 1B) indicate that the thickness of some silcrete lenses must have exceeded 1.5 m (*14*). Similarly, little is known about the original extent of sarsen deposits. Prehistoric and later stoneworkers used sarsen for structures including prehistoric monuments, Roman villas, medieval churches, and farm buildings, and in road construction (*29*). The long-axis length of surviving boulders rarely exceeds 4.0 to 5.0 m (*22*), and none reaches the size of the Stonehenge megaliths.

Despite historical extraction, it is still possible to identify the most likely provenance of the sarsens at Stonehenge by using a geochemical fingerprinting approach to characterize the chemistry of remaining boulder scatters. Sarsens in southern Britain developed through the silicification of a range of sedimentary units (*22*), including various sandy Paleogene formations and, in Norfolk, the Cretaceous Greensand. These formations have been shown to exhibit distinctive and regionally variable heavy mineral assemblages [e.g., (*30*)]. By inference from silcrete provenancing studies in southern Africa (*20*, *21*) and Australia (*31*), this should mean that the remaining sarsens in different areas will exhibit different inherited heavy mineral assemblages and, hence, different chemistries.

To assess the chemical variability within British sarsens, we sampled boulders (with landowner permission) in 20 representative areas of sarsen concentration. This included sites from Devon in the west to Norfolk in the east (Fig. 1 and table S2). Areas dominated by conglomeratic silcrete (locally called "puddingstone") were not sampled, as this material is not present at Stonehenge. Greatest attention was paid to Wiltshire, with six areas sampled in the Marlborough Downs alone; these include three on the highest points of the Downs (sites 1, 2, and 6 in Fig. 1B) and three lower-lying "sarsen trains" within chalk dry valleys (sites 3 to 5). Stones at each site were selected at random, and three ~100-g samples of sarsen were collected using a geological hammer and chisel. Each of these samples was analyzed by ICP-MS/-AES using the same analytical protocol as applied to the Phillips' Core samples from Stonehenge (see data file S1 for full dataset).

Like the Phillips' Core samples, the geochemistry of the sarsens in different areas of Britain is dominated by silica and therefore records very little variability in the major elements. However, differences in trace element geochemistry, controlled by the nonquartz mineralogy of the stone, can be identified. To quantify these differences, we calculated Zr-normalized trace element ratios to produce geochemical signatures for each of the 20 sarsen sampling areas (see Materials and Methods). Data for individual trace elements were used only if that element (i) is normally immobile in near-surface weathering environments (*32*, *33*), (ii) was measured with an instrumental precision of 1 part per million (ppm) or better, and (iii) was recorded at or above detection limits in at least two of the three analyses per site. The resulting signatures (Fig. 3) reflect both within-site chemical variability and instrumental uncertainty.

To determine the most likely source area for Stone 58 (and hence the majority of the Stonehenge sarsens), we compared the median immobile trace element signature for the Phillips' Core with the 20 site-specific geochemical signatures (Fig. 3). In semianalogous geochemical studies [e.g., (*34*)], the typical approach used to "match" chemical fingerprints relies on simple visual comparison of the shape of the trace element signatures of potentially cogenetic rocks to prove provenance. In the case of Stonehenge, such a simple comparison is insufficient, given the subtle differences in trace element chemistry between some of the potential source areas.

For there to be a permissible match between the immobile trace element signature for Stone 58 and a potential source area, we argue that all the trace element ratios for the Phillips' Core must lie within the limits of instrumental uncertainty of that area. As shown in Fig. 3, the geochemical signature for the Phillips' Core exhibits a poor match for all sites beyond the Marlborough Downs (sites 7 to 20 on Fig. 1), with disparities evident for two or more of the 21 trace element ratios calculated for each site. It is therefore highly unlikely that Stone 58 was sourced from these areas. On the same basis, we can discount five of the six sampling localities within the Marlborough Downs (sites 1 to 5) as potential sources; this includes Piggledene, identified previously as an unlikely source region on the basis of heavy mineral analyses (*11*).

The remaining site, West Woods, in the southeast Marlborough Downs, yields permissible matches for all median immobile trace element ratios from the Phillips' Core; this includes Pr/Zr, U/Zr, and La/Zr, which fall within instrumental uncertainty. We can therefore conclude that, based on our data, Stone 58 and, hence, the majority of the sarsens used to construct Stonehenge were most likely sourced from the vicinity of West Woods. Archaeological investigations and further detailed sampling of sarsens from West Woods and surrounding areas are now required to more tightly constrain the precise source area(s) and identify prehistoric sarsen extraction pits.

DISCUSSION

Overlooking the Kennet Valley to the north, West Woods covers a ~6-km^2 area and comprises a plateau rising to 220 m above sea level that is dissected by two narrow valleys. The area once contained a dense concentration of sarsens, including a sarsen train mapped by the Ordnance Survey as recently as 1924. Most of the stones were broken up and removed from the mid-19th century onward. However, many large boulders remain, both in valleys and on high ground, and sarsen extraction pits are common, particularly in the northern woodland (*35*, *36*). West Woods lies within a concentration of Early Neolithic activity, being close to Avebury, numerous long barrows, and the causewayed enclosure at Knap Hill (*37*).

Fig. 3. Zr-normalized immobile trace element ratio data for 20 sarsen localities across southern Britain and the Phillips' Core from Stone 58 at Stonehenge. Data ranges for each of the sarsen localities are indicated by the pink shaded region on each plot. The upper (lower) boundary for each area is defined by the maximum (minimum) Zr-normalized ratio calculated for each element plus (minus) 3 SD of instrumental uncertainty. The solid black line is the median value for each Zr-normalized ratio from the three analyses of the Phillips' Core. The maximum (minimum) error bars represent plus (minus) 3 SD of instrumental uncertainty.

Evidence of Mesolithic through Iron Age occupation has been recorded in the area, including a 40-m-long Early Neolithic chambered long barrow, sarsen standing stones, a sarsen *polissoir* used to sharpen stone axes, and prehistoric fields where now-wooded ground was previously open, cultivated land (*36*, *38*, *39*).

Why, in a region with the greatest density of extant sarsen stones in Britain (Fig. 1A), West Woods was selected as the primary source for the Stonehenge sarsens is unclear. Its significance most likely derives from the size and quality of the stones present there, making the area an important location for Neolithic people (*37*). Its topographic position on high ground south of the Kennet and its relative proximity to Salisbury Plain would also have made it an efficient place from which to obtain the sarsens. West Woods is located ~3 km south of the area where the majority of antiquaries and archaeologists have looked for Stonehenge's sarsen quarries [e.g., (*14*, *40*)] and, thus, lies slightly closer to the monument at ~25 km in a direct line. Only the antiquary John Aubrey had previously postulated a link between "Overton Wood," probably a former name of West Woods, and Stonehenge (*41*).

The identification of a single source area for the majority of the sarsens at Stonehenge and the chemical consistency across the different structural components of the monument support previous suggestions that the stones were all erected at much the same time [around 2500 BCE, during the monument's second stage of construction; (*13*)]. It had been proposed, based on its large size and undressed nature, that the Heel Stone (Stone 96) was a natural sarsen from the immediate vicinity of Stonehenge that was erected early in the history of the monument (*13*). Our PXRF data, however, show that Stone 96 has a similar chemical composition to most other sarsens at Stonehenge, which suggests that it, too, was brought from West Woods.

Our results further help to constrain the most likely route along which the sarsens were transported to Stonehenge. Atkinson (*42*) chose a route that headed southwest from a source area near Avebury and then south toward Salisbury Plain, while Hill (*5*) proposed an alternative route along the River Avon (Fig. 1B). A more recent reappraisal (*43*) used an origin north of the River Kennet, a crossing of the river at Clatford, and then a journey northwest of West Woods, down into the Vale of Pewsey beside Knap Hill, across the River Avon at Marden and then southward to climb the scarp slope of Salisbury Plain at its most gentle incline. Atkinson's route can now be dismissed. However, as our sarsen samples were collected from the western side of West Woods, a route from West Woods via Knap Hill could be appropriate (Fig. 1B). If stones were also sourced from the eastern woods, then an alternative route might run 2 km to the east, along what is now the White Horse Trail, dropping down to the Vale of Pewsey, and then along the River Avon close to Hill's proposed route.

Why Stones 26 and 160 were obtained from different source areas from the other sarsens at Stonehenge is intriguing. Both lie at the northernmost points of their respective arrays: Stone 26 is the northernmost upright of the Sarsen Circle, and Stone 160 the lintel of the northernmost trilithon. While this could be coincidental, one possibility is that their presence marks out the work of different builder communities who chose to source their materials from a different part of the landscape. A similar theory has been proposed for the digging of separate segments of the surrounding ditch at Stonehenge (*43*). We cannot discount the possibility that Stones 26 and 160 were sourced relatively close to the monument site. However, ICP-MS/-AES analyses from these stones and sarsen samples from locations closer to Stonehenge are required to confirm or refute this. It is possible that some of the ~28 stones missing from the Sarsen Circle and peripheral settings were also derived from these different source areas, but we will probably never know.

MATERIALS AND METHODS

Method used for PXRF analysis

PXRF analyses of each of the 52 extant sarsen stones at Stonehenge were undertaken using an Olympus Innov-X Delta Professional Portable XRF device. The model operates at 40 kV, is equipped with an Rh anode 4-W x-ray tube, and uses a Silicon Drift Detector. The "Geochem" mode, which captures Mg, Al, Si, P, S, K, Ca, Ti, V, Cr, Mn, Fe, Co, Ni, Cu, Zn, As, Se, Rb, Sr., Y, Zr, Nb, Mo, Ag, Cd, Sn, Sb, W, Hg, Pb, Bi, U, and Th, was used for all analyses. The instrument has a detector window approximately 20 mm in diameter, while the x-ray source excites a target circle with a 3-mm diameter.

PXRF analyses of standing and fallen sarsen uprights and fallen lintel stones (see Fig. 1D) were undertaken by authors D.J.N. and T.J.R.C. from ground level. Analyses of the nine in situ sarsen lintel stones were undertaken by T.J.R.C. from a mobile scaffold tower provided courtesy of English Heritage. Five points that were as flat as possible and free of lichen cover were selected on the surface of each sarsen stone. Each point was analyzed for 120 s of total exposure. The device was positioned such that the PXRF detector window was completely covered by the stone. At the start/end of analyses and after every 15 analyses (i.e., three stones), a calibration check was made against a 316 Stainless Steel Calibration Check Reference Coin to ensure accuracy and consistency of the results. All data were processed in Microsoft Excel. The full PXRF dataset for this investigation is available in Worksheet 1 of data file S1.

Method used for ICP-MS and ICP-AES analyses

Three subsamples of sarsen from the Phillips' Core plus three samples from each of the 20 sarsen localities across southern Britain (Fig. 1) were processed and analyzed by ALS Minerals (Seville, Spain). Any weathered outer surface material present on the 20 field samples was removed using a rock saw before dispatch to Spain. In Spain, each sample/subsample was first crushed using a hardened steel jaw crusher such that >70% of the resulting fragments passed through a 2-mm screen size (ALS Geochemistry preparation package CRU-31). The crushed samples were then powdered in an agate ball mill such that >85% passed a 75-μm screen size (ALS Geochemistry package PUL-42). Major and minor oxides were analyzed by lithium metaborate fusion digestion and ICP-AES (ALS Geochemistry method ME-ICP06). Trace elements, including rare earth elements, were determined using lithium metaborate fusion digestion and ICP-MS (ALS Geochemistry method ME-MS81). As, Bi, Hg, In, Re, Sb, Se, and Te were determined by aqua regia digestion, followed by ICP-MS (ALS Geochemistry method ME-MS42). Ag, Cd, Co, Cu, Li, Mo, Ni, Pb, Sc, and Zn were determined by four-acid digestion and ICP-AES (ALS Geochemistry method ME-4ACD81).

In all cases, ICP-MS analyses were conducted using an Elan 9000 instrument and ICP-AES analyses using a Varian 700 Series instrument. Total C and S were analyzed by Leco induction furnace and Leco sulfur analyzer (ALS Geochemistry methods C-IR07 and S-IR08, respectively). Loss on ignition (LOI) was calculated following ignition of sample powders at 1000°C (ALS Geochemistry method

OA-GRA05). The full ICP-MS and ICP-AES data for this investigation, including Certified Reference Materials (CRMs) and blank and repeat analyses, are available in Worksheets 2 and 3 of data file S1.

Generation of Zr-normalized trace element ratios from ICP-MS/-AES data

To generate the geochemical signatures presented in Fig. 3, we use ICP-MS/-AES data only for trace elements that (i) are normally immobile in near-surface weathering environments, (ii) were measured with an instrumental precision of 1 ppm or better, and (iii) were recorded at or above detection limits in at least two of the three analyses per site. These trace elements are Ba, Ce, Dy, Er, Gd, Hf, Ho, La, Nb, Nd, Pr, Rb, Sm, Sr, Tb, Th, Ti, Tm, U, Y, and Yb.

For all samples, the concentrations (ppm) of the listed elements were each divided by the concentration (ppm) of Zr for the same sample to yield a set of unitless Zr-normalized trace element ratios. The Zr-normalized trace element ratios for the three samples from each site define maximum, median, and minimum values for that site. An equivalent set of Zr-normalized trace element ratios was calculated for the three samples from the Phillips' Core (SHCORE1 to 3), with the median values used to define the solid black line in Fig. 3.

During the acquisition of geochemical data, four separate CRMs were analyzed by ALS Minerals in the sample batch pursuant to the ICP-MS and ICP-AES data presented here. The GRE-3 and SY-4 CRMs were analyzed twice each, while OREAS-122 and REE-1 were both analyzed five times. The results of these 14 CRM analyses and the published values for the four CRMs are shown in Worksheet 3 of data file S1.

The differences between the published CRM values and our 14 CRM analyses were used to plot the *y* axis error bars for the Phillips' Core and define the compositional range for each of the 20 sarsen sampling areas shown in Fig. 3. To do this, the percentage difference in trace element concentration between the published values and our analyses was calculated for each CRM to give a measure of analytical uncertainty (%) for each element. We then summed the analytical uncertainty (%) for each element and the analytical uncertainty (%) for Zr to give the analytical uncertainty (%) for each Zr-normalized trace element ratio. The SD (σ) in analytical uncertainty (%) for each Zr-normalized trace element ratio was then calculated from the resulting data. To define the maximum (minimum) errors bars for the Phillips' Core, three times this percentage value was added to (subtracted from) each median Zr-normalized trace element ratio. To define the compositional range for each of the 20 sarsen sampling areas, three times this percentage value was added to (subtracted from) the maximum (minimum) Zr-normalized trace element ratio derived for each site. The resulting values define the upper and lower boundaries for the shaded regions for each site shown in Fig. 3. The full workings for the derivation of analytical uncertainty are shown in Worksheet 4 of data file S1.

Statistical analysis

Both LDA and BPCA are commonly used dimensionality reduction techniques. These techniques were applied to 250 of the 260 individual PXRF readings from Stonehenge. Ten readings were excluded as they contained anomalously low (<75%) Si once the PXRF data had been normalized to 100% to remove the light element fraction (data file S1). Only the following 26 elements from the PXRF dataset were included in the statistical analyses: Mg, Al, P, S, K, Ti, V, Cr, Mn, Ni, Cu, Zn, As, Rb, Sr, Y, Zr, Nb, Mo, Ag, W, Hg, Pb, Bi, Th, and U. Where any element was recorded at below detection limits ("ND" in data file S1), it was treated as an unknown value. Si, Ca, and Fe were excluded to avoid potential anomalies caused by the introduction of iron and replacement of Si by Ca during late-stage diagenesis and subaerial weathering. Co, Cd, Se, Sb, and Sn were below detection limits in all PXRF readings; as such, these elements cannot be used as discriminatory variables and were also excluded.

LDA was applied to the PXRF dataset using the R statistical suite (*44*) and specifically the default lda() function. For the analysis, PXRF readings were grouped by stone. Eighty percent of the dataset was used for training. Results are presented in Fig. 2A. While showing clear clustering, the LDA model has limited interpretational value, as the first two discriminant functions combined explain <60% of the variance in the dataset. As such, no further breakdown of LDA results is presented.

BPCA was applied to the PXRF dataset using the pcaMethods R package (*45*). BPCA was selected over standard PCA on the basis that the technique can handle >10% of unknown values in a dataset; the pcaMethods R package was specifically developed for treating incomplete datasets. The results of BPCA (Fig. 2B) explain 95% of the dataset between the first two principal components. The covariance between the first six principal components is shown in fig. S1, and the element loadings for each of these principal components are shown in table S2. BPCA performs an automated calculation for dimensionality.

SUPPLEMENTARY MATERIALS

Supplementary material for this article is available at http://advances.sciencemag.org/cgi/content/full/6/30/eabc0133/DC1

REFERENCES AND NOTES

1. W. Lambarde, *Dictionarium Angliae Topographicum et Historicum: An Alphabetical Description of the Chief Places in England and Wales; with an Account of the Most Memorable Events Which Have Distinguish'd Them* (F. Gyles, London, 1730).
2. W. Stukeley, *Stonehenge a Temple Restr'd to the British Druids* (W. Innys and R. Manby, London, 1740).
3. W. Gowland, J. W. Judd, III.—Recent excavations at Stonehenge. *Archaeologia* **58**, 37–118 (1902).
4. H. H. Thomas, The source of the stones of Stonehenge. *Antiquaries J.* **3**, 239–260 (1923).
5. P. A. Hill, The sarsens of Stonehenge: The problem of their transportation. *Geogr. J.* **127**, 488–492 (1961).
6. G. A. Kellaway, Glaciation and the stones of Stonehenge. *Nature* **232**, 30–35 (1971).
7. R. E. Bevins, R. A. Ixer, N. J. G. Pearce, Carn Goedog is the likely major source of Stonehenge doleritic bluestones: Evidence based on compatible element geochemistry and Principal Component Analysis. *J. Arch. Sci.* **42**, 179–193 (2014).
8. T. Darvill, G. Wainwright, Beyond Stonehenge: Carn Menyn Quarry and the origin and date of bluestone extraction in the Preseli Hills of south-west Wales. *Antiquity* **88**, 1099–1114 (2014).
9. M. Parker Pearson, J. Pollard, C. Richards, K. Welham, C. Casswell, C. French, D. Schlee, D. Shaw, E. Simmons, A. Stanford, R. E. Bevins, R. A. Ixer, Megalith quarries for Stonehenge's bluestones. *Antiquity* **93**, 45–62 (2019).
10. R. Ixer, R. Bevins, D. Pirrie, P. Turner, M. Power, No provenance is better than wrong provenance: Milford Haven and the Stonehenge sandstones. *Wilts. Arch. Nat. Hist. Soc. Mag.* **113**, 1–15 (2020).
11. H. Howard, A petrological study of the rock specimens from excavations at Stonehenge, 1979–1980, in On the road to Stonehenge: Report on the investigations beside the A344 in 1968, 1979 and 1980, by M.W. Pitts. *Proc. Prehist. Soc.* **48**, 104–124 (1982).
12. D. J. Nash, J. S. Ullyott, Silcrete, in *Geochemical Sediments and Landscapes*, D. J. Nash, S. J. McLaren, Eds. (Blackwell, Oxford, 2007), pp. 95–143.
13. T. Darvill, P. Marshall, M. Parker Pearson, G. Wainwright, Stonehenge remodelled. *Antiquity* **86**, 1021–1040 (2012).
14. M. Parker Pearson, The sarsen stones of Stonehenge. *Proc. Geol. Assoc.* **127**, 363–369 (2016).
15. M. Abbott, H. Anderson-Whymark, *Stonehenge Laser Scan: Archaeological Analysis Report* (English Heritage Research Report 32-2012, Swindon, 2012).

16. H. C. Bowen, I. F. Smith, Sarsen stones in Wessex: The society's first investigations in the evolution of the landscape project. *Antiquaries J.* **57**, 185–196 (1977).
17. C. P. Green, The provenance of rocks used in the construction of Stonehenge. *Proc. Brit. Acad.* **92**, 257–270 (1997).
18. J. M. D. Day, Determining the source of silcrete sarsen stones. *J. Arch. Sci. Rep.* **28**, 102051 (2019).
19. K. A. Whitaker, What if none of the building stones at Stonehenge came from Wiltshire? *Oxford J. Arch.* **38**, 148–163 (2019).
20. D. J. Nash, S. Coulson, S. Staurset, J. S. Ullyott, M. Babutsi, L. Hopkinson, M. P. Smith, Provenancing of silcrete raw materials indicates long-distance transport to Tsodilo Hills, Botswana, during the Middle Stone Age. *J. Hum. Evol.* **64**, 280–288 (2013).
21. D. J. Nash, S. Coulson, S. Staurset, J. S. Ullyott, M. Babutsi, M. P. Smith, Going the distance: Mapping mobility in the Kalahari Desert during the Middle Stone Age through multi-site geochemical provenancing of silcrete artefacts. *J. Hum. Evol.* **96**, 113–133 (2016).
22. M. A. Summerfield, A. S. Goudie, The sarsens of southern England: their palaeoenvironmental interpretation with reference to other silcretes, in *The Shaping of Southern England*, D. K. C. Jones, Ed. (Academic Press, London, 1980), pp. 71–100.
23. J. S. Ullyott, D. J. Nash, Micromorphology and geochemistry of groundwater silcretes in the eastern South Downs, UK. *Sedimentology* **53**, 387–412 (2006).
24. M. A. Summerfield, Origin and palaeoenvironmental interpretation of sarsens. *Nature* **281**, 137–139 (1979).
25. C. M. Bishop, Bayesian PCA, in *Advances in Neural Information Processing Systems 11 (NIPS 1998)*, M. J. Kearns, S. A. Solla, D. A. Cohn, Eds. (1998), pp. 382–388.
26. M. M. Herron, Geochemical classification of terrigenous sands and shales from core or log data. *J. Sed. Res.* **58**, 820–829 (1988).
27. R. J. Small, M. J. Clark, J. Lewin, The periglacial rock-stream at Clatford Bottom, Marlborough Downs, Wiltshire. *Proc. Geol. Assoc.* **81**, 87–98 (1970).
28. J. S. Ullyott, D. J. Nash, C. A. Whiteman, R. N. Mortimore, Distribution, petrology and mode of development of silcretes (sarsens and puddingstones) on the eastern South Downs, UK. *Earth Surf. Proc. Landf.* **29**, 1509–1539 (2004).
29. N. E. King, The Kennet Valley sarsen industry. *Wilts. Arch. Nat. Hist. Mag.* **63**, 83–93 (1968).
30. A. C. Morton, The provenance and diagenesis of Palaeogene sandstones of southeast England as indicated by heavy mineral analysis. *Proc. Geol. Assoc.* **93**, 263–274 (1982).
31. G. W. G. Cochrane, J. A. Webb, T. Doelman, P. J. Habgood, Elemental differences: Geochemical identification of aboriginal silcrete sources in the Arcadia Valley, eastern Australia. *J. Arch. Sci. Rep.* **15**, 570–577 (2017).
32. J. J. Middelburg, C. H. van der Weijden, J. R. W. Woittiez, Chemical processes affecting the mobility of major, minor and trace elements during weathering of granitic rocks. *Chem. Geol.* **68**, 253–273 (1988).
33. J. A. Pearce, A user's guide to basalt discrimination diagrams, in *Trace Element Geochemistry of Volcanic Rocks: Appliction for Massive Sulphide Exploration*, D. Wyman, Ed. (Geological Association of Canada, Mineral Deposits Division, Winnipeg, 1996), pp. 79–113.
34. R. E. Ernst, W. Bleeker, U. Söderlund, A. C. Kerr, Large Igneous Provinces and supercontinents: Toward completing the plate tectonic revolution. *Lithos* **174**, 1–14 (2013).
35. K. A. Whitaker, Sarsen stone quarrying in southern England: An introduction, in *Mining and Quarrying in Neolithic Europe: A Social Perspective,* A. Teather, P. Topping, J. Baczkowski, Eds. (Neolithic Study Group Seminar Papers 16, Oxbow Books, Oxford, 2019), pp. 101–113.
36. L. Amadio, *West Woods, Wiltshire: An Archaeological Survey* (Wiltshire Archaeological and Natural History Society, Devizes, 2011); https://wiltshireafg.weebly.com/uploads/1/5/5/1/15516698/167-0304-1_west_woods.pdf.
37. M. Gillings, J. Pollard, Making megaliths: Shifting and unstable stones in the Neolithic of the Avebury landscape. *Camb. Arch. J.* **26**, 537–559 (2016).
38. A. D. Passmore, Chambered long barrow in West Woods. *Wilts. Arch. Nat. Hist. Mag.* **42**, 49–51 (1923).
39. P. J. Fowler, *Landscape plotted and pieced. Landscape history and local archaeology in Fyfield and Overton, Wiltshire* (Society of Antiquaries of London, London, 2000).
40. T. Darvill, *Stonehenge: The Biography of a Landscape* (Tempus, Stroud, 2006).
41. J. Aubrey, *The Natural History of Wiltshire* (Wiltshire Topographical Society, London, 1847).
42. R. J. Atkinson, *Stonehenge* (Hamish Hamilton, London, 1956).
43. M. Parker Pearson, *Stonehenge: Exploring the Greatest Stone Age Mystery* (Simon and Schuster, London, 2013).
44. R Core Team, *R: A Language and Environment for Statistical Computing* (R Foundation for Statistical Computing, Vienna, Austria, 2013); www.R-project.org/.
45. W. Stacklies, H. Redestig, M. Scholz, D. Walther, J. Selbig, pcaMethods—A bioconductor package providing PCA methods for incomplete data. *Bioinformatics* **23**, 1164–1167 (2007).
46. H. C. Brentnall, Sarsens. *Wilts. Arch. Nat. Hist. Mag.* **51**, 419–439 (1946).
47. D. K. C. Jones, Evolving models of the Tertiary evolutionary geomorphology of southern England, with special reference to the chalklands in *Uplift, Erosion and Stability, Special Publication 162*, W. B. Whalley, B. J. Smith, M. Widdowson, Eds. (Geological Society, London, 1999), pp. 1–24.

Acknowledgments: We would like to thank the following: H. Sebire (English Heritage) for authorizing site access to Stonehenge; landowners, including the National Trust and Forestry Commission, for permission to sample individual sarsen localities; M. Allfrey (English Heritage) for permission to sample the core from Stone 58; J. Shaw and R. Turley (University of Bristol) for subsampling the core from Stone 58; M. Higgins (Open University) for sample preparation; and ALS Minerals (Seville, Spain) for ICP-MS/-AES characterization of sarsen samples. **Funding:** Fieldwork and analyses were supported by the British Academy/Leverhulme Trust Small Research Grant SG170610—"Geochemical fingerprinting the sarsen stones at Stonehenge." **Author contributions:** Conceptualization and funding acquisition—D.J.N., T.J.R.C., J.S.U., M.P.P., and T.D.; methodology and validation—D.J.N., T.J.R.C., G.M., and S.G.; investigation—D.J.N., T.J.R.C., J.S.U., G.M., S.G., K.A.W.; statistical analysis—G.M. and D.J.N.; other formal analysis—all authors; writing (original draft)—D.J.N., T.J.R.C., G.M., M.P.P., T.D., S.G., K.A.W.; writing (review and editing)—all authors; project administration and data curation—D.J.N. **Competing interests:** The authors declare that they have no competing interests. **Data and materials availability:** All data needed to evaluate the conclusions in the paper are present in the paper and/or the Supplementary Materials.

Submitted 1 April 2020
Accepted 10 June 2020
Published 29 July 2020
10.1126/sciadv.abc0133

Citation: D. J. Nash, T. J. R. Ciborowski, J. S. Ullyott, M. P. Pearson, T. Darvill, S. Greaney, G. Maniatis, K. A. Whitaker, Origins of the sarsen megaliths at Stonehenge. *Sci. Adv.* **6**, eabc0133 (2020).

Science Advances

Origins of the sarsen megaliths at Stonehenge

David J. Nash, T. Jake R. Ciborowski, J. Stewart Ullyott, Mike Parker Pearson, Timothy Darvill, Susan Greaney, Georgios Maniatis and Katy A. Whitaker

Sci Adv **6** (31), eabc0133.
DOI: 10.1126/sciadv.abc0133